UNCONVENTIONAL ELECTRONIC AND MAGNETIC PROPERTIES OF sp^2 / sp^3 MIXED DISORDERED CARBON

K.Takai[1], M.Oga[1], S. Aoki[1], T.Enoki[1], A. Taomoto[2], Y. Ohki[2]
[1] *Department of Chemistry, Tokyo Institute of Technology, Ookayama, Meguro, Tokyo, 152-8551, Japan.*
[2] *Matsushita Electric Industrial Co., Ltd., Higashimita, Tama-ku, Kawasaki, 214-8501, Japan.*
Corresponding author e-mail address:ktakai@chem.titech.ac.jp

Introduction

In the most cases of disordered carbons that are defined as sp^2 / sp^3 mixed carbon, the increase in the sp^2-carbon ratio causes clustering of sp^2-sites and tends to develop graphitic structure, which favors the itinerant electron character as confirmed by high conductivity and large diamagnetism. From opposite point of view, the graphitic structure featured with hexagonal π-electron planar network is easily destroyed and is converted to a sp^2 / sp^3 mixture with atomic-scale disorder by introducing even a comparatively small concentration of sp^3-bonds, when sp^3-sites are homogeneously distributed in space. The absence of graphitic structure in such sp^2 / sp^3 mixture seems to bring about non-conductive nature. However, tight-binding and *ab initio* calculations claim a large density of states at the Fermi energy $D(E_F)$ that originates from gapless electronic structure of the non-graphitic but sp^2-rich sp^2 / sp^3 mixture, where the graphitic hexagonal network is absent [1,2]. In the present study, the structure and electronic properties of sp^2-rich non-graphitic sp^2 / sp^3 -mixed carbon, are investigated in terms of the heat-treatment (HT) and transition metal-doping effects.

Experimental

Samples were prepared by PLD by Nd:YAG laser (532 nm, 0.14 W / mm) with a HOPG target in vacuum. HT of the samples was performed for 30 min under 1×10^{-6} Torr. For convenience, the samples heat-treated at xx00 °C will be labeled “HTT xx00”, and non-heat-treated sample is labeled “non-HT” hereafter. The samples doped with transition metals were prepared by PLD using a carbon-metal composite target. The structure and electronic properties of the prepared samples were examined by means of X-ray diffraction (XRD), Raman spectrum, electron energy loss spectroscopy (EELS), electric conductivity, thermoelectric power, magnetic susceptibility, ESR measurements.

Results and Discussion

1. Structural Change upon Heat-Treatment

In XRD profiles shown in Fig. 1, the absence of any peak suggests that the samples for HTT < 600 °C do not have any regularity in their structure even in the atomic-scale range. In the mean time, EELS measurement verifies that even the non-HT sample has almost 90 % of sp^2-carbon atoms, and sp^2 / sp^3 ratio is preserved upon HT up to HTT 1300 [3]. Therefore, the samples in the low-HTT region are sp^2-rich disordered carbon without graphitic structure. Graphitic diffraction peak (00*n*) grows in the range HTT >

600 ºC, accompanied with the increase of its peak intensity and the decrease of their peak linewidth upon the elevation of HTT. This suggests that graphitic structure becomes important in the local structure upon the elevation of HTT. Interestingly, the temperature range, in which the structural change toward graphitic structure occurs, is considerably lowered in comparison with a typical temperature ~1200 ºC for the conversion from the sp^3-carbon to sp^2 one [4]. This proves that, in the non-HT sample, the sp^2 / sp^3 mixed structure having atomic-scale disorder with 10 % sp^3-sites is in a thermodynamically non-equilibrium state and tends to be easily relaxed to graphitic state which is thermodynamically well defined. Such non-graphitic structural nature of the non-HT sample and the rapid development of graphitic structure with slight annealing are also confirmed in the Raman experiments. In the enough high temperature region (HTT>1300 ºC), the conversion from sp^3-carbon to sp^2-carbon is responsible for the development of graphitic structure.

2. Electronic Transport Properties

The HT-induced development of the graphitic structure tends to extend the hexagonal-networked π-plane areas. As a result, the developed graphite π-bands become to fill the π - π* gap, and the $D(E_F)$ increases as HTT increases. Figures 2 and 3 show the temperature dependence of the electrical conductivity and the thermoelectric power of the samples at various HTTs. The conductivity increases accompanied with an insulator-metal transition around HTT~1100 °C as HTT is elevated. The strong random potential produced by defects is considered to make the electronic states localized, resulting in the insulating feature in the low HTT region. A sharp increase of the conductivity upon HT for HTT < 600 °C is attributed to the consequence of the structural

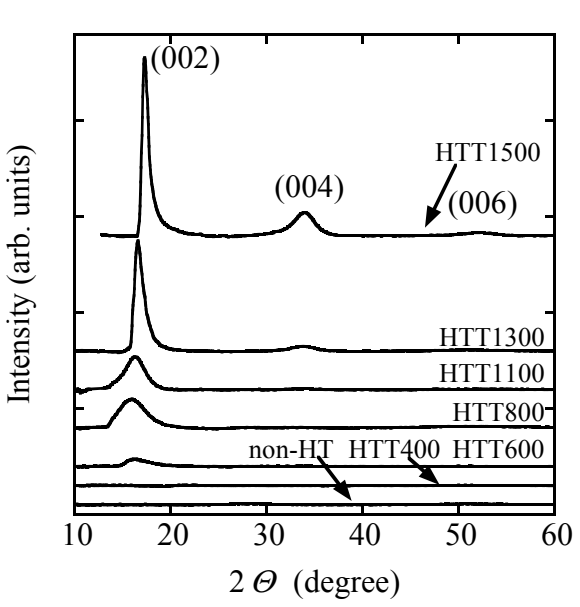

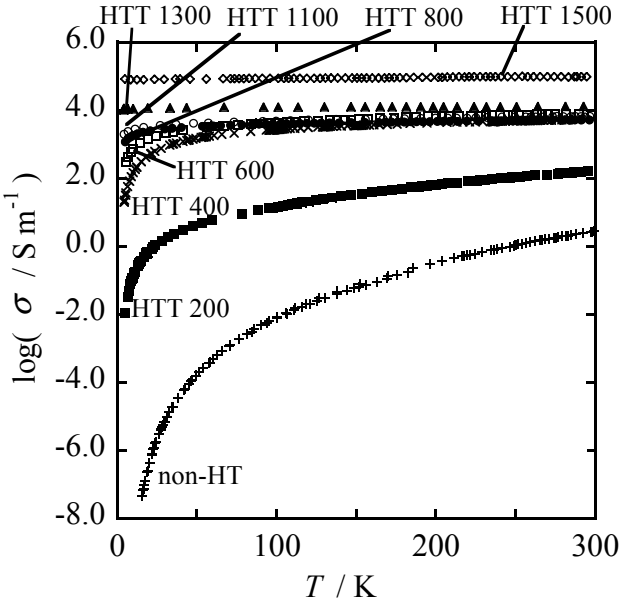

Figure 1. (left) XRD patterns of the samples at various HTTs. The base lines of the patterns are shifted vertically from each other for clarify.
Figure 2. (right) The temperature dependence of the electrical conductivity.

relaxation from the non-equilibrium state. In the insulating region, there is a crossover in the conductivity behavior around HTT 200 - 400 °C, below and above which ln σ obeys linear relation with $T^{-1/4}$ and $T^{-1/2}$, respectively. This suggests that the electron transport process is governed by the 3D variable hopping process at low HTTs below the crossover point, whereas the carrier correlation plays an important role above the crossover point. The raise in the $D(E_F)$ and the enhancement in the structural regularity induced by HT increase the carrier density and mean free path in the conduction process, respectively, resulting in the steep elevating in the conductivity and changing in the temperature dependence of the conductivity.

The thermoelectric power for HTT 200 exhibits a comparably large thermoelectric power over 10 $\mu V \cdot K^{-1}$ at room temperature, while it is insensitive to HTT and extremely small (~1 $\mu V \cdot K^{-1}$ at room temperature) in the high HTT region (HTT > 400 °C) The change in the thermoelectric power is considered to be caused also by the increase in $D(E_F)$ around 400 < HTT < 600 °C. The thermoelectric power in the higher HTT region can be explained by taking the spatial inhomogeneity of the sample into consideration. There coexist metallic and insulating domains randomly distributed in space with various sizes and structures. In such systems, the thermoelectric power is given by the sum of the contributions from both kinds of domains. The contribution of insulating domains makes thermoelectric power diverge at low temperatures, while the metallic domains give linear temperature-dependent thermoelectric power at high temperatures. Moreover, the Fermi levels are distributed depending on metallic domains as well as the energy gaps in insulating domains. This leads to spatial fluctuations in the positions of the E_F. In this situation, each metallic domain is positively or negatively charged up through mutual charge transfer so as to achieve consistency with the net remaining charges, which are related to the mean E_F in the whole system. Eventually, both domains with hole carriers and electron carriers coexisting cause the carrier compensation.

3. Magnetic Properties

The temperature dependence of the magnetic susceptibility for the non-HT and HTT 600 samples is shown in Fig. 4. Both of them behave as the combination of the two components; temperature dependent Curie-Weiss term χ_c and temperature independent term χ_0. The localized spin density N_s is calculated as 2.2×10^{20} spin / g from the Curie constant and Weiss temperature Θ is obtained as -5 K for the non-HT sample. The origin of the Curie paramagnetism is attributed to the localization of the electrons induced by the random potential originating from the atomic-scale disorder nature of the non-HT sample. The negative Weiss temperature suggests the presence of antiferromagnetic interaction between the localized spins, which is also evidenced by the magnetization curve. With an assumption of the homogeneous distribution of the localized spins, the average distance between the localized spins is calculated as 1.7 nm, which is too long for the direct exchange interaction between the spins. The long-range exchange interaction mediated by itinerant electrons is suggested.

Transition metal doping confirms a mediating role of π-electrons in the exchange interaction mechanism. Actually, for the Ni-doped samples, the presence of additional magnetic moments of 0.1 spin / Ni atom is proved from the susceptibility behavior. However, the magnetization curve at 2 K shows the similar behavior to that of the non-

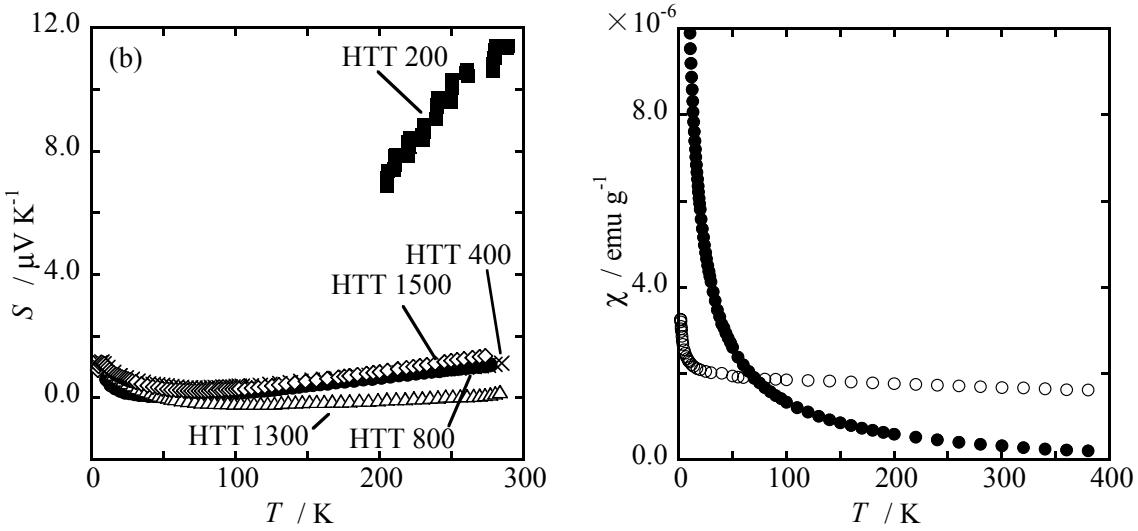

Figure 3. (left) The temperature dependence of the thermoelectric power of the samples at various HTTs.
Figure 4. (right) The temperature dependence of the susceptibility for the non-HT and HTT 600 samples. Closed circles and open circles denote the non-HT and HTT 600 samples, respectively.

doped sample, which suggests the complete quenching of localized spins of the nickel origin in the low temperature. It is confirmed that the doping induces no difference in the structural feature of the host carbon network from the non-doped sample according to information from Raman spectra. Taking the atomic composition ratio (Ni / Ci ~ 0.6 %) into consideration, the average distance between Ni-spins is too far for direct exchange interaction. Accordingly, the π-electron mediated antiferromagnetic interaction is suggested between nickel d-electron spins.

The temperature independent term χ_0 is more suggestive of the existence of itinerant electron in the sp^2-rich non-graphitic carbon systems. In ordinary gaphitic disordered carbon systems, χ_0 usually takes the negative value due to the orbital diamagnetism contribution, since the Pauli paramagnetism χ_P is negligible because of its negligible $D(E_F)$ of the graphitic band (~10^{-8} emu g^{-1}). On the other hand, the large contribution of χ_P to the observed positive χ_0 is expected for the non-HT sample. In addition, HT raises the Pauli susceptibility as evidenced by the behavior of HTT 600 shown in Fig. 4. Indeed, χ_P is estimated as 1.8×10^{-6} emu / g for HTT 600 sample, which is in the similar range to that of alkaline metals (~ 10^{-6} emu / g) rather than that of graphitic materials (at the most, 6.4×10^{-7} emu g^{-1}, for KC_8 [5]). The ESR signal confirms the large contribution of temperature independent Pauli paramagnetic component for the non-HT sample.

The coexistence of the Pauli paramagnetism at high temperatures and the Curie-type behavior at low temperatures in the samples is explained in terms of electron correlation. According to theory, both electron correlation and disorder play important roles in the electron localization in Anderson insulator system [6]. Especially, in the strongly disordered system, where the localization length is enough small, the interstate

Coulomb interactions are negligible in comparison with intrastate interactions. The singly occupied states originating from intrastate electron correlation gives Curie-type behavior at low temperatures, where intrastate interaction is enough larger than thermal energy. In the high temperature region, the Curie contribution gradually diminishes and eventually, only the Pauli paramagnetism of degenerated electrons at E_F appears. At HTT 600, N_s is about three orders of magnitudes smaller than that of the non-HT sample as estimated from the result in Fig. 4. The increase in the localization length induced by the development of the structural regularity upon HT diminishes the localization nature of the electron spins. The enhancement of the Pauli paramagnetism at HTT 600 is consistent with this situation.

Conclusions

The structures and electronic properties are investigated for sp^2-rich non-graphitic sp^2 /sp^3 carbon prepared by PLD. The non-HT sample is in thermodynamically non-equilibrium state with atomic-scale disorder, where the structure is completely modified from that of graphite in spite of sp^2-rich system. The electronic structure of the non-HT sample, being far from that of graphitic band structure, has a large $D(E_F)$. Although the strong random potential makes most of electrons localized, a small concentration of itinerant electrons contributes to the long-range exchange interaction and the large Pauli paramagnetism at high temperatures. In the meantime, on-site Coulomb repulsion causes the Curie-type magnetism at low temperatures. Because of the meta-stable structural nature of the non-graphitic sp^2 /sp^3 carbon, even slight HT causes a conversion from non-graphitic to graphitic structure. The developed structural regularity makes the electrons itinerant, which is responsible for enhancement of the Pauli paramagnetism, the electric conductivity, and the carrier correlation effects in the conduction mechanism at the expense of the Curie paramagnetism at low temperature.

Acknowledgments

The present work was supported by the Grant-in-Aid for "Research for the Future Program", Nano-carbons, and the Grant-in-aid for Scientific Research No. 13440208 and 15105005 from JSPS.

References

[1] J. Robertson, E. P. O'Reilly, Electronic and atomic structure of amorphous carbon Phys. Rev. B, 1987; 35(6) 2946-2957.
[2] N. A. Marks, D. R. McKenzie, B. A. Pailthorpe, M. Bernasconi, and M. Parrinello, Phys. Rev. Lett., Microscopic Structure of Tetrahedral Amorphous Carbon 1996; 76(5) 768-771.
[3] K. Takai, M. Oga, H. Sato, T. Enoki, Y. Ohki, A. Taomoto, K. Suenaga, S. Iijima, Structure and electronic properties of a nongraphitic disordered carbon system and its heat-treatment effects, Phys. Rev. B, 2003; 67(21) 214202-214212.
[4] Pierson HO. Handbook of Carbon, Graphite, Diamond and Fullerenes. Park Ridge NJ: Noyes. 1993; 257.
[5] M. S. Dresselhaus, G. Dresselhaus, Intercalation compounds of graphite, Adv. in Phys., 1981; 30(2) 139-326.
[6] H. Kamimura, Impurity Bands in: P. N. Butcher, N. H. March, and M. P. Tosi, editor, Crystalline Semiconducting Material and Devices, Plenum Press, 1986; 305-354.